
Chemical Thermodynamics of Uranium in the Soil Environment

Michael Thomas Aide

Additional information is available at the end of the chapter

<http://dx.doi.org/10.5772/intechopen.72107>

Abstract

Uranium is present in the soil environment because of human activity, including the usage of U-bearing phosphorus fertilizers. In oxic and many suboxic soil environments, U(VI) is the dominant uranium valence species. With pH, pe (Eh), the partial pressure of CO₂, the mineralogy of the adsorbing surfaces and the uranium concentration as the key master variables, U(VI) will predictably participate in hydrolysis, ion-pairing, complexation, ion-exchange, mineral precipitation and adsorption reactions. An extensive listing of thermochemical data is currently available for detailed simulations to assist with model setup, data interpretation and system understanding. In this chapter, simulations of U(VI) hydrolysis with variable pCO₂ activities, U(IV) and U(VI) precipitation, U(VI) reduction and U(VI) complexation with carbonate and phosphate assemblages illustrate the usefulness and applicability of simulations in data analysis and experimental design.

Keywords: uranium hydrolysis, uranium complexation, uranium adsorption, simulation, soil

1. Properties, sources, characteristics of soil uranium

Uranium is the third element in the actinide series having an atomic number of 92 and an electronic configuration of [Rn] 5f³6d¹7s². The 5f orbitals are less effective in penetrating the inner core electrons than the 4f orbitals (lanthanide series), thus permitting more favored covalent bonding character [1]. Uranium(IV) and uranium(VI) have ionic radii of 89 and 73 pm, respectively. The two, more abundant, long-lived isotopes of uranium are ²³⁵U₉₂ and ²³⁸U₉₂. The naturally occurring mass abundances of uranium isotopes are ²³⁴U (0.0057%), ²³⁵U (0.71%) and ²³⁸U (99.284%). ²³⁵U is fissile, whereas ²³⁸U in a breeder reactor will yield fissile ²³⁹Pu [2].

Uranium decay is an isotope function, with (i) ^{238}U decaying by α -emission to $^{234}\text{Th}_{90}$ (half-life of 4.45×10^9 years) and then by two successive β -emissions (half-life of 24.1 days and half-life of 1.18 minutes) to yield ^{234}U . ^{234}U will undergo α -emission (half-life of 2.45×10^5) to yield $^{230}\text{Th}_{90}$, whereas ^{235}U decaying by α -emission to yield ^{231}Th (half-life of 7.04×10^8 years) and later in the decay sequence to yield ^{227}Th [2].

2. Introduction to soil uranium

The Earth's crustal uranium abundance is centered near 2.3 mg U/kg [1]. Soil parent materials vary substantially in their uranium concentrations, with granites (4.4 mg U/kg) and shales (3.8 mg U/kg) having greater abundances than basalts (0.8 mg U/kg) and K-feldspars (1.5 mg U/kg) [3]. The phyllosilicates, muscovite and biotite have U concentrations centering near 20 mg U/kg, and some zircon minerals may have up to 2500 mg U/kg [3]. Aide et al. [4] documented total uranium concentrations by soil horizon depth in numerous southeastern Missouri soils, noting that the uranium concentrations varied from 0.58 to 2.89 mg U/kg, with course-textured soils generally having smaller U concentrations. In their study, uranium in individual soil pedons was well correlated with Fe-oxyhydroxide concentrations. Birke et al. [5] reported that the amount of uranium in river waters in Germany varied from 0.007 to 43.7 $\mu\text{g U/L}$, with a median of 0.33 $\mu\text{g U/L}$. Mendez-Garcia et al. [6] observed that high uranium concentrations in sediment in the Rio Grande Basin in Mexico were of natural occurrence.

Common uranium-bearing minerals include: uraninite [UO_2], pitchblende [U_3O_8], coffinite [$\text{U}(\text{SiO}_4)_{1-x}(\text{OH})_{4x}$], brannerite [UTi_2O_6], davidite [(rare earth elements) (Y,U) (Ti,Fe $^{3+}$) 20 O_{38}] and thucholite [uranium-bearing pyrobitumen]. Less abundant uranium-bearing minerals include: autunite [$\text{Ca}(\text{UO}_2)_2(\text{PO}_4)_2 \bullet 8\text{--}12 \text{ H}_2\text{O}$], carnotite [$\text{K}_2(\text{UO}_2)_2(\text{VO}_4)_2 \bullet 1\text{--}3 \text{ H}_2\text{O}$], selecite [$\text{Mg}(\text{UO}_2)_2(\text{PO}_4)_2 \bullet 10 \text{ H}_2\text{O}$], torbernite [$\text{Cu}(\text{UO}_2)_2(\text{PO}_4)_2 \bullet 12 \text{ H}_2\text{O}$], tyuyamunite [$\text{Ca}(\text{UO}_2)_2(\text{VO}_4)_2 \bullet 5\text{--}8 \text{ H}_2\text{O}$], uranocircite [$\text{Ba}(\text{UO}_2)_2(\text{PO}_4)_2 \bullet 8\text{--}10 \text{ H}_2\text{O}$], uranophane [$\text{Ca}(\text{UO}_2)_2(\text{HSiO}_4)_2 \bullet 5 \text{ H}_2\text{O}$], zeunerite [$\text{Cu}(\text{UO}_2)_2(\text{AsO}_4)_2 \bullet 8\text{--}10 \text{ H}_2\text{O}$], rutherfordine [UO_2CO_3] and schoepite [$(\text{UO}_2)_8\text{O}_2(\text{OH})_2 \bullet 12\text{H}_2\text{O}$]. Uranium(V) species and associated minerals are comparatively rare because of disproportionation into U(IV) and U(VI) species [1].

Soils may become uranium impacted because of nuclear fuel production, nuclear weapons production, depleted uranium in munitions, coal combustion and most importantly by phosphorus fertilizer applications [7–19]. Stojanovic et al. [17] observed that maize and sunflower plants may be very useful for uranium phytoremediation, with the root mass acquiring much greater uranium accumulations than culms, leaves and grain. Stojanovic et al. [18] documented previous research showing that the use of phosphorus fertilizers may contribute 73% of the total anthropogenic uranium to the global soil resource. Echevarria et al. [20] observed that low pH levels favored increased uranium plant availability. Laroche et al. [21] in a hydroponic study observed that phosphorus reduced uranyl activity, especially at higher pH intervals.

Plant uptake of U has been investigated for phytoremediation of impacted soils [7, 13–15, 22–34]. Sunflower (*Helianthus annuus*) has been shown to substantially phytoaccumulate U(VI)

[33]. Sheppard et al. [30] noted that leafy vegetables could accumulate U(VI) to a greater extent than common grain crops. Chopping and Shambhag [35] showed U(VI) binding by soil organic matter, particularly if the soil organic materials acquired a negative charge density at or above pH 7. Organic complexes of U may be replaced by other cations, especially divalent and trivalent cations [36].

Phyllosilicates (clay minerals) typically manifest a net negative charge density because of isomorphous substitution and unsatisfied edge charges [36–38]. Al-, Mn- and Fe-oxyhydroxides have variable charged surfaces (amphoteric) that acquire a positive charge density when the pH is more acidic than the mineral's point of zero net charge density [39, 40]. Uranyl ions, along with its hydroxyl monomers and hydroxyl polymers, will participate in adsorption reactions with phyllosilicates and Mn- and Fe-oxyhydroxides [41–49]. The transport of U-bearing colloids by wind and water erosion is an important source of U transport from impacted sites.

There lies great interest in understanding the U transport in natural systems such as soil profiles, sediments and aquifers [4, 9, 10, 19, 40, 50–52]. Johnson et al. [51] investigated depleted uranium soil sites in Nevada (USA), observing that uranium retention is a function of (1) soil type, (2) soil binding site concentrations, (3) the presence of phyllosilicates and their associated Fe-oxyhydroxides, (4) the contaminant concentration, (5) the presence of competing ions and (6) the contaminant speciation based on pH and Eh. They noted that the estimated distribution coefficients (K_d = concentration of the sorbed contaminant/the contaminant in the aqueous phase) increased with soil reaction from pH 7 to pH 11. Roh et al. [16] investigated two U-impacted sites at Oak Ridge, TN using sequential leaching and demonstrated that soil U was associated substantially with carbonates (45%) and Fe-oxyhydroxides (40%).

3. Uranium hydrolysis

Hydrolysis constants for U(IV) are presented in **Table 1**.

The solubility of U(IV) may be estimated from thermochemical data, with the assumption that UO_2 is the crystalline phase, as: $UO_2 + 2H_2O + OH^- = U(OH)_5^-$.

($\log K_{s,1,5} = -3.77$).

$U^{4+} + H_2O = U(OH)^{3+} + H^+$	$\log K_{1,1} = -0.65$
$U^{4+} + 2H_2O = U(OH)_2^{2+} + 2H^+$	$\log K_{1,2} = -0.2.6$
$U^{4+} + 3H_2O = U(OH)_3^+ + 3H^+$	$\log K_{1,3} = -5.8$
$U^{4+} + 4H_2O = U(OH)_4 + 4H^+$	$\log K_{1,4} = -10.3$
$U^{4+} + 5H_2O = U(OH)_5^- + 5H^+$	$\log K_{1,5} = -16.0$
$6U^{4+} + 15H_2O = U_6(OH)_{15}^{9+} + 15H^+$	$\log K_{6,15} = -17.2$

Table 1. Hydrolysis constants for U(IV) (Baes and Mesmer [53]).

	Baes and Mesmer [53]	Davis [54]
$\text{UO}_2^{2+} + \text{H}_2\text{O} = \text{UO}_2(\text{OH})^+ + \text{H}^+$	$\log K_{1,1} = -5.8$	$= -5.20$
$\text{UO}_2^{2+} + 2\text{H}_2\text{O} = \text{UO}_2(\text{OH})_2 + 2\text{H}^+$	—	$= -11.50$
$\text{UO}_2^{2+} + 3\text{H}_2\text{O} = \text{UO}_2(\text{OH})_3^- + 3\text{H}^+$	—	$= -20.00$
$\text{UO}_2^{2+} + 4\text{H}_2\text{O} = \text{UO}_2(\text{OH})_4^{2-} + 4\text{H}^+$	—	$= -33.00$
$2\text{UO}_2^{2+} + 1\text{H}_2\text{O} = (\text{UO}_2)_2(\text{OH})_1^{3+} + \text{H}^+$	—	$= -2.70$
$2\text{UO}_2^{2+} + 2\text{H}_2\text{O} = (\text{UO}_2)_2(\text{OH})_2^{2+} + 2\text{H}^+$	$\log K_{2,2} = -5.62$	$= -5.62$
$3\text{UO}_2^{2+} + 5\text{H}_2\text{O} = (\text{UO}_2)_3(\text{OH})_3^+ + 5\text{H}^+$	$\log K_{3,5} = -15.63$	$= -15.55$

Table 2. Hydrolysis constants for U(VI) [53, 54].

The uranyl ion (UO_2^{2+}) is an oxyanion, given that the high charge polarization of U^{6+} prevents this aqueous species from being stable. Hydrolysis constants for U(VI) are presented in **Table 2**.

In low ionic strength media, the U(VI) polymers are not thermodynamically favored, with the exception of $(\text{UO}_2)_3(\text{OH})_3^+$ [41, 42, 44, 46, 49, 54–58].

4. Simulation of uranium hydrolysis

Using the MinteqA2 software [59], U(VI) speciation may be estimated from thermochemical data for pH intervals from pH 4 to pH 8. Setting the total U(VI) concentration at 10^{-8} mole/liter, the pCO_2 pressure at 0 and then again at 0.02 bar (2 kPa) were the primary model variable inputs. Establishing a constant ionic strength with 0.01 mole NaNO_3 /liter, activity coefficients were estimated using the Debye-Huckel equation. In the CO_2 closed system, UO_2^{2+} is the dominant species in very acidic media, whereas $\text{UO}_2(\text{OH})^+$ is the dominant species from pH 6 to pH 8 (**Table 3**). The ion pair UO_2NO_3^+ is an important secondary species, particularly in acidic media. In the CO_2 open system, UO_2^{2+} is the dominant species in very acidic media; however, the UO_2CO_3 , $\text{UO}_2(\text{CO}_3)_2^{2-}$ and $\text{UO}_2(\text{CO}_3)_3^{4-}$ are U(VI) species increasingly dominant upon transition from acidic media to neutral and then to alkaline media (**Table 3**). Importantly, the uranyl carbonate complexes are stable at Eh conditions that would promote U(VI) reduction in CO_2 closed systems. This MinteqA2 simulation of dilute U(VI) speciation closely corresponds with the analytical data and its MinteqA2 simulation as presented by Langmuir [38] and also the data analysis from Waite et al. [58].

Repeating the simulation at 10^{-3} mol U/L, with allowance for mineral precipitation yielded different U species distributions across the pH intervals (**Table 4**). At pH 4, the UO_2^{2+} species is increasingly converted by polymerization into the $(\text{UO}_2)_2(\text{OH})_2^{2+}$ species. At pH 5, the UO_2^{2+} and UO_2CO_3 species similarly transitioned into the $(\text{UO}_2)_3(\text{OH})_3^+$ and the $(\text{UO}_2)_2(\text{OH})_2^{2+}$ species. The pH 7 and 8 simulations witnessed the expanding abundances of $\text{UO}_2(\text{CO}_3)_2^{2-}$. Rutherfordine (UO_2CO_3) was indicated to have precipitated at pH 4–7, whereas calcite (CaCO_3) precipitated at pH 8.

Species	-log (activity)				
	pH 4	pH 5	pH 6	pH 7	pH 8
UO ₂	8.21 (96.8%)	9.5 (44.8%)	10.3	13.6	19.2
UO ₂ (OH)	10.1	9.4 (4.1%)	10.2	12.5	17.1
(UO ₂) ₂ (OH) ₂	14.0	12.7	14.2	18.8	27.9
(UO ₂) ₃ (OH) ₅	20.2	16.2	16.6	21.4	33.1
UO ₂ NO ₃	10.0 (1.2%)	10.3	12.1	15.4	20.9
UO ₂ CO ₃	9.9 (1.1%)	8.3 (50.3%)	8.1 (83.8%)	9.4 (4.3%)	
UO ₂ (CO ₃) ₂	14.9	11.2	9.0 (14.8%)	8.3 (77.8%)	9.9 (2.5%)
UO ₂ (CO ₃) ₃	22.2	16.5	12.3	9.6 (17.9%)	9.1 (97.5%)

Total U concentration was 10⁻⁸ mole/L.

Activity coefficients were determined by the Debye-Huckel equation.

The presence of CO₂(g) at 2 × 10⁻² bar (2 kPa) and an ionic strength standardized by 0.01 M NaNO₃. Calcium concentrations were 0.001 mol/L. Within a pH column, () indicates the percentage of the U species.

Table 3. The MinteqA2 simulation of U(VI) speciation.

Species	-log (activity)				
	pH 4	pH 5	pH 6	pH 7	pH 8
UO ₂	2.61 (38.1%)	4.6 (14.5%)	6.6	8.6	13.6
UO ₂ (OH)	4.51	5.5 (1.3%)	6.5	7.5	11.7
(UO ₂) ₂ (OH) ₂	2.79 (49.8%)	4.8 (19%)	6.8	8.8	17.1
(UO ₂) ₃ (OH) ₅	3.41 (11.1%)	4.4 (48.6%)	5.4 (19.8%)	6.4	16.9
UO ₂ NO ₃	4.39	6.4	8.4	10.4	15.6
UO ₂ CO ₃	4.36	4.4(16.4%)	4.4 (66.6%)	4.4 (4%)	7.5
UO ₂ (CO ₃) ₂	9.31	7.3	5.3 (11.8%)	3.3 (75.8%)	4.5
UO ₂ (CO ₃) ₃	16.6	12.6	8.6	4.6 (20.0%)	3.7 (99.5%)

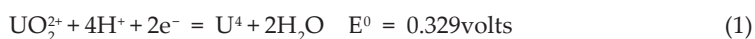
Total U concentration was 10⁻³ mole/L, which was allowed to equilibrate and allow precipitation.

Calcium concentrations were standardized at 10⁻³ mole/L. The presence of CO₂ (g) at 2 × 10⁻² bar (2 × 10³ pascal) and an ionic strength standardized by 0.01 M NaNO₃. Within a pH column, () indicates the percentage of the U species. Activity coefficients were determined by the Debye-Huckel equation. Rutherfordine (UO₂CO₃) was predicted to precipitate from pH 4 to pH 7, whereas calcite was predicted to precipitate at pH 8.

Table 4. The MinteqA2 simulation of U(VI) solubility by species in the presence of CO₂ (g).

5. Uranium oxidation and reduction

The reduction of U(VI) to U(IV) may be presented as [53]:



At Eh values less than 0.2 volts, U(VI) reduction to uraninite (UO_2) is favored. Stewart et al. [60] observed that U(VI) reduction to U(IV) is inhibited in the presence of ferrihydrite. Yajima et al. [61] also observed that U(VI) reduction to U(IV) limited mobility. Goldhaber et al. [62] observed that coffinite formed via reduction processes in sedimentary rocks. Fendorf et al. [63] reviewed the biotic and abiotic pathways for U(VI) reduction in anaerobic soils, and they noted that U(IV) has more limited mobility and binds more preferentially to substrates than U(VI). Uranyl reduction is facilitated by bacterially mediated reactions [64]; however, non-crystalline ferric oxides and nitrate may be effective terminal electron acceptors. Similarly, Burgos et al. [63] observed that soil humic acid partially inhibits U(VI) reduction.

6. Simulation of uranium reduction

At a pe of 5 (296 mv), indicative of suboxic soil redox conditions, and at a total U concentration of 10^{-8} mol/L, the MinteqA2 simulation of U(VI) reduction to U(IV) indicates that U(IV) would

Species	-log (activity)				
	pH 4	pH 5	pH 6	pH 7	pH 8
U(VI) Speciation					
UO_2	8.2 (98.6%)	8.5 (44.8%)	10.3	13.6	19.2
$\text{UO}_2(\text{OH})$	10.1	9.4 (4.1%)	10.2	12.5	17.1
$(\text{UO}_2)_2(\text{OH})_2$	14.0	12.7	14.2	18.8	27.9
$(\text{UO}_2)_3(\text{OH})_5$	20.2	16.2	16.6	21.4	33.1
UO_2NO_3	10.0 (1.2%)	10.3	12.0	15.4	21.0
UO_2CO_3	10.0 (1.1%)	8.3 (50.5%)	8.1 (83.8%)	9.4 (4.3%)	12.9
$\text{UO}_2(\text{CO}_3)_2$	14.9	11.3	9.0 (14.8%)	8.3 (77.8%)	9.9 (2.5%)
$\text{UO}_2(\text{CO}_3)_3$	22.2	16.5	12.3	9.6 (17.9%)	9.1 (97.5%)
U(IV) Speciation					
U^{4+}	25.0	29.3	35.1	42.4	52.0
$\text{U}(\text{OH})$	21.7	25.0	29.8	36.0	44.6
$\text{U}(\text{OH})_2$	19.3 (1.6%)	21.6	25.4	30.7	44.6
$\text{U}(\text{OH})_3$	17.9 (24.1%)	19.3 (1.1%)	22.0	26.3	32.9
$\text{U}(\text{OH})_4$	17.1 (58.7%)	17.8 (26.9%)	19.6 (3.6%)	22.9	28.5
$\text{U}(\text{OH})_5$	18.1 (15.7%)	17.4 (72.0%)	18.2 (96.4%)	20.5 (99.6%)	25.1 (100%)

Total U concentration was 10^{-8} mole/L, which was allowed to equilibrate and allow reduction at a pe of 5 (296 mv). Activity coefficients were determined by the Debye-Huckel equation.

Calcium concentrations were standardized at 10^{-3} mole/L. The presence of CO_2 (g) at 2×10^{-2} bar (2×10^3 pascal) and an ionic strength standardized by 0.01 M NaNO_3 . Within a pH column, () indicates the percentage of the U species.

Table 5. The MinteqA2 simulation of U(VI) reduction to U(IV) in the presence of CO_2 (g) at 2×10^{-2} bar (2 kilopascal) and an ionic strength standardized by 0.01 M NaNO_3 .

U(VI) Speciation	-log (activity)	U(IV) Speciation	-log (activity)
UO ₂	19.9	U ⁴⁺	28.7
UO ₂ (OH)	19.8	U(OH)	23.3
(UO ₂) ₂ (OH) ₂	33.3	U(OH) ₂	18.9
(UO ₂) ₃ (OH) ₅	45.2	U(OH) ₃	15.6
UO ₂ NO ₃	21.6	U(OH) ₄	13.2 (3.6%)
UO ₂ CO ₃	17.6 (83.7%)	U(OH) ₅	11.8 (96.4%)
UO ₂ (CO ₃) ₂	18.6 (14.8%)		
UO ₂ (CO ₃) ₃	21.8		

Total U concentration was 10⁻³ mole/L, which was allowed to equilibrate and allow reduction at a pe of -3 (-177 mv). Activity coefficients were determined by the Debye-Huckel equation. Calcium and sulfate were present initially at 0.001 mole/L. Uraninite was precipitated and established the U equilibria (saturation index 0.00). No carbonate, sulfate or sulfide minerals were documented to precipitate. Calcium concentrations were standardized at 10⁻³ mole/L. The presence of CO₂ (g) at 2 × 10⁻² bar (2 × 10³ pascal) and an ionic strength standardized by 0.01 M NaNO₃. Within a column, () indicates the percentage of the U species.

Table 6. The MinteqA2 simulation of U(VI) reduction to U(IV) in the presence of CO₂ (g) at pH 6 at a pe of -3 (-177 mv).

be undetectable by inductively coupled plasma emission spectroscopy-mass spectroscopy or other comparable analytical technologies (Table 5). At pH 4, the dominant U(IV) species was U(OH)₄⁻, whereas at pH 5–8, the dominant species was U(OH)₅⁻. The dominant U(VI) species were UO₂ (pH 4), UO₂ and UO₂CO₃ (pH 5), UO₂CO₃ (pH 6), UO₂(CO₃)₂ (pH 7) and UO₂(CO₃)₃ (pH 8).

At a pe of -3 (-177 mv), indicative of anoxic soil redox conditions, and at a total U concentration of 10⁻³ mole/L at pH 6, the simulation of U(VI) reduction to U(IV) indicates that the dominant U(IV) species was U(OH)₅⁻ (Table 6). The dominant U(VI) species were UO₂CO₃ (83.7%) and UO₂(CO₃)₂ (14.8%). The MinteqA2 predicted that uraninite(UO₂) formed as a solid phase.

7. Uranium complexation with an emphasis on phosphorus

Uranium complexation pairs a central cation (coordination center) with a surrounding array of molecules and ions. Phosphorus interactions with U(VI) have been studied to assess whether phosphorus may reduce the availability and mobility of U(VI) [12, 65–67]. Stojanovic et al. [18] reported that phosphorus may readily form uranyl phosphates and subsequently precipitate autunite. They noted that at pH levels greater than 6.0, the dominant U(VI)-phosphorus species was the plant-available UO₂PO₄ species, whereas at more acidic soil reactions, UO₂HPO₄ and UO₂H₂PO₄⁺ were more abundant and are not considered as plant-available U-phosphate species. Grabias et al. [65] studied uranyl acetate immobilization in ferruginous soils amended with phosphates. In acidic pH ranges, a strong U(VI) sorption was observed in the presence of phosphate, supporting their premise that adsorption was promoted by the formation of UO₂(H₂PO₄)(H₃PO₄)⁺, UO₂(H₂PO₄)₂ and (UO₂)₃(PO₄)₃·4H₂O.

Mehta et al. [67] demonstrated that U(VI) flux in soil columns was substantially reduced when phosphate was present. Sequential extractions demonstrated that the U(VI) could be readily extracted by ion-exchange and dilute acid treatments. Laser-induced fluorescence spectroscopy inferred adsorption to be the dominant retention mechanism.

Sandino and Bruno [68] determined the solubility of $(\text{UO}_2)_3(\text{PO}_4)_2 \cdot 4\text{H}_2\text{O}$ (s) and the formation of U(VI) phosphate complexes over the pH range of pH 4–9. In their study, UO_2HPO_4 and UO_2PO_4^- were the dominant U species. Minimum U(VI) solubility for the $(\text{UO}_2)_3(\text{PO}_4)_2 \cdot 4\text{H}_2\text{O}$ (s) system occurred near pH 6, whereas the minimum U(VI) solubility for amorphous (non-crystalline) and crystalline schoepite occurred near the pH levels of pH 7.4 and 8.4, respectively. Thermodynamic data for U(VI) with respect to phosphate and carbonate from the literature are well-documented by Sandino and Bruno [68].

Lenhart et al. [69] described uranium(VI) complexation with citric acid, humic acid and fulvic acid in acidic media (pH 4.0 and 5.0). Using Schubert's ion-exchange method, the U(VI)-citric acid complex was determined to be 1:1 uranyl-citrate complex ($\beta_{1,1} = 6.69 \pm 0.3$ at $I = 0.10$). Humic and fulvic acids were demonstrated to strongly bind to U(VI), with humic acid forming a slightly stronger binding complex. The U(VI)-humic acid and U(VI)-fulvic acid complexes were determined to be non-integral (1 U(VI) with between 1 and 2 humic or fulvic acids), suggesting that a 1:1 stoichiometry involving a limited number of high-affinity sites.

Ivanov et al. [70] observed uranyl sorption on bentonite in the presence of humic acid with trace levels of uranium(VI). Uranyl sorption on bentonite was shown to be strongly pH dependent. In the absence of humic acid, U(VI) sorption exhibited a sorption edge between pH 3.2 and pH 4.2. In the presence of humic acid, U(VI) sorption slightly increased at low pH and curtails at moderate pH. Soluble uranyl carbonate species inhibited U(VI) sorption at alkaline pH levels. At pH intervals from pH 3 to pH 4, UO_2HA was predicted ($[\text{U}] = 8.4 \times 10^{-11}$ and $p\text{CO}_2 = 10^{-3.5}$ atm, HA = humic acid). From pH 5 to pH 7, $\text{UO}_2(\text{OH})\text{HA}$ was predicted to be the dominant species. Tinnacher et al. [71] studied the reaction kinetics of tritium-labeled fulvic acid on uranium(VI) sorption onto silica, demonstrating that metal sorption rates are a complex function of metal and organic ligand concentrations and the nature and abundance of mineral surface sites.

$2\text{UO}_2^{2+} + 3\text{H}_2\text{O} + \text{H}_2\text{CO}_3 = (\text{UO}_2)_2\text{CO}_3(\text{OH})_3^- + 5\text{H}^+$	$\log K = -17.54$
$\text{UO}_2^{2+} + \text{H}_2\text{CO}_3 = \text{UO}_2\text{CO}_3 + 2\text{H}^+$	$\log K = -7.01$
$\text{UO}_2^{2+} + 2\text{H}_2\text{CO}_3 = \text{UO}_2(\text{CO}_3)_2^{2-} + 4\text{H}^+$	$\log K = -16.43$
$\text{UO}_2^{2+} + 3\text{H}_2\text{CO}_3 = \text{UO}_2(\text{CO}_3)_3^{4-} + 6\text{H}^+$	$\log K = -28.45$
$\text{UO}_2^{2+} + \text{NO}_3^- = \text{UO}_2\text{NO}_3^+$	$\log K = 0.30$
$\text{H}^+ + \text{CO}_3^{2-} = \text{HCO}_3^-$	$\log K = -6.35$
$2\text{H}^+ + \text{CO}_3^{2-} = \text{H}_2\text{CO}_3$	$\log K = -16.68$

Table 7. Formation constants for selected aqueous species (Davis [44]).

$\text{UO}_2^{2+} + 2\text{H}_2\text{O} = \text{UO}_2(\text{OH})_2 + 2\text{H}^+$	$\log K = -5.4$
$\text{UO}_2^{2+} + \text{CO}_3^{2-} = \text{UO}_2\text{CO}_3$	$\log K = 14.11$
$2\text{UO}_2^{2+} + \text{Ca}^{2+} + 2\text{PO}_4^{3-} = \text{Ca}(\text{UO}_2)_2(\text{PO}_4)_2$	$\log K = 48.61$
$2\text{UO}_2^{2+} + \text{Fe}^{2+} + 2\text{PO}_4^{3-} = \text{Fe}(\text{UO}_2)_2(\text{PO}_4)_2$	$\log K = 46.00$
$\text{UO}_2^{2+} + \text{H}^+ + \text{PO}_4^{3-} = \text{H}(\text{UO}_2)\text{PO}_4$	$\log K = 25.00$

Table 8. Precipitation reactions involving U(VI) (Chen and Yiacoumi [40]).

Reaction	$\log \beta$
$\text{UO}_2^{2+} + \text{H}_3\text{PO}_4 = \text{UO}_2\text{H}_3\text{PO}_4^{2+}$	0.76 ± 0.15
$\text{UO}_2^{2+} + \text{H}_3\text{PO}_4 = \text{UO}_2\text{H}_2\text{PO}_4^+ + \text{H}^+$	1.12 ± 0.07
$\text{UO}_2^{2+} + 2\text{H}_3\text{PO}_4 = \text{UO}_2(\text{H}_3\text{PO}_4)\text{H}_2\text{PO}_4^+ + \text{H}^+$	1.69 ± 0.15
$\text{UO}_2^{2+} + 2\text{H}_3\text{PO}_4 = \text{UO}_2(\text{H}_2\text{PO}_4)_2 + \text{H}^+$	0.87 ± 0.05

H_3PO_4 Ka1, Ka2 and Ka3 constants are (-2.14 ± 0.03) , (-7.21 ± 0.02) and (-12.35 ± 0.03) , respectively.

Table 9. Experimental equilibrium data for the U(VI)- H_3PO_4 at $I = 0$ (Grenthe et al. [55]).

Sandino and Bruno [68] reported the oxalate and sulfate complexation reactions involving the uranyl cation: (1) $\text{UO}_2^{2+} + \text{Oxalate}^{2-} = \text{UO}_2\text{Oxalate}$, $\log \beta = 6.02$ and (2) $\text{UO}_2^{2+} + \text{Sulfate}^{2-} = \text{UO}_2\text{Sulfate}$, $\log \beta = 1.92$. Tandy et al. [72] reported that citrate and malate from root exudates supported greater uranium concentrations in the adjacent soil solution. Sandino and Bruno [68] provided phosphate complexation reactions involving the uranyl cation: (1) $\text{UO}_2^{2+} + \text{HPO}_4^{2-} = \text{UO}_2\text{HPO}_4$, $\log \beta = 7.28 \pm 0.10$ and (2) $\text{UO}_2^{2+} + \text{PO}_4^{3-} = \text{UO}_2\text{PO}_4^{1-}$, $\log \beta = 13.25 \pm 0.09$. Additional equilibrium constants are presented in **Tables 7–9**.

8. Simulation of uranium complexation with H_3PO_4

The MinteqA2 simulation of U(VI) at 10^{-3} mol U/L demonstrated that the dominant U(VI)-phosphate species were $\text{UO}_2(\text{HPO}_4)_2$ at pH 4 and 6, whereas at pH 8, the dominant species were $\text{UO}_2(\text{CO}_3)_3^{4-}$ (67.9%) and $\text{UO}_2(\text{HPO}_4)_2$ (30.6%). Rutherfordine and $(\text{UO}_2)_3(\text{PO}_4)_2$ were formed as solid phases (**Table 10**).

Species	-log (activity)		
	pH 4	pH 6	pH 8
UO_2	5.3 (3.1%)	7.3	14.4
$\text{UO}_2(\text{OH})$	7.2	7.2	12.3
$(\text{UO}_2)_2(\text{OH})_2$	8.2	8.2	18.4
$(\text{UO}_2)_3(\text{OH})_5$	11.5	7.5	18.9

Species	-log (activity)		
	pH 4	pH 6	pH 8
UO ₂ NO ₃	7.1	9.0	16.1
UO ₂ HPO ₄	6.4	7.4	11.0
UO ₂ (HPO ₄) ₂	3.8 (98.4%)	3.8 (96.0%)	3.8 (30.6%)
UO ₂ H ₂ PO ₄	7.2	10.2	15.8
UO ₂ (H ₂ PO ₄) ₂	10.1	14.1	18.1
UO ₂ (H ₂ PO ₄) ₃	13.3	18.3	20.7
UO ₂ PO ₄	8.8	7.8	9.4
UO ₂ CO ₃	7.1	5.1 (3.3%)	8.2
UO ₂ (CO ₃) ₂	12.0	6.0	5.1 (1.5%)
UO ₂ (CO ₃) ₃	19.3	9.3	4.4 (67.9%)

Total U concentration was 10⁻³ mole/L, which was allowed to equilibrate and allow precipitation of rutherfordine and (UO₂)₃(PO₄)₂.

Activity coefficients were determined by the Debye-Huckel equation.

Calcium and H₃PO₄ concentrations were initially standardized at 10⁻³ mole/L. The presence of CO₂ (g) at 2 × 10⁻² bar (2 kPa) and an ionic strength standardized by 0.01 M NaNO₃. Within a pH column, () indicates the percentage of the U species.

Table 10. The MinteqA2 simulation of U(VI) species in the presence of CO₂ (g) and H₃PO₄.

9. Uranium solubility and precipitation

The solubility of U(VI) may be estimated from thermochemical data with the assumption that UO₂(OH)₂ is the crystalline phase [53] as:



Hsi and Langmuir [56] investigated the adsorption of U(VI) onto noncrystalline Fe(OH)₃ and goethite (α-FeOOH) in batch 0.1 mole NaNO₃/liter suspensions prepared with different total carbonate concentrations and pH intervals. Hsi and Langmuir documented that the optimum adsorption pH was near pH 6.3–6.5 for noncrystalline Fe(OH)₃ and in alkaline media, U(VI)-carbonate complexes effectively reduced U(VI) adsorption. The effect of carbonate in the goethite suspensions broadened the pH of maximum U(VI) adsorption from pH 5.7 to pH 8.0, a feature attributed to the lack of U(VI)-carbonate complex desorption. Waite et al. [58] investigated U(VI) adsorption onto hydrous ferric oxides, noting that the maximum U(VI) adsorption occurred from pH 5 to pH 9; however, in the presence of carbonate, the U(VI) adsorption in the pH interval from pH 8 to pH 9 was limited. In general, U(VI) adsorption into Fe-oxyhydroxides is greater than phyllosilicate minerals.

Typically, the pH range of minimal U(VI) mineral solubility coincides with the pH range for optimal U(VI) adsorption. U(IV) complexes are frequently less soluble and less mobile than U(VI) complexes [73]. Duquene et al. [23] noted that U(VI) reduction to less soluble U(IV), by either biotic or abiotic processes, influenced uranium mobility. Stojanovic et al. [17] confirmed that soil temperature, pH, oxidation–reduction potentials and the presence of complexing agents were important factors influencing uranium bioavailability and plant uptake. Shahandeh and Hossner [33] employed a selective sequential extraction protocol to show that U(VI) partitioned into exchangeable, carbonate, manganese, iron, organic and residual fractions. In soils where the carbonate fraction was expected to be important, appreciable plant uptake of U(VI) into the roots and culms of a wide variety of plants was demonstrated. In soils having U(VI) partitioning into iron, manganese and organic fractions, the U(VI) plant uptake was substantially smaller.

Sandino and Bruno [68] provided the solubility estimate for $(\text{UO}_2)_3(\text{PO}_4)_2 \cdot 4\text{H}_2\text{O}(\text{s}) = 3\text{UO}_2^{2+} + 2\text{PO}_4^{3-} + 4\text{H}_2\text{O}$ as $\log K_{\text{so}} \pm 2\sigma = 48.48 \pm 0.16$.

10. Uranium adsorption

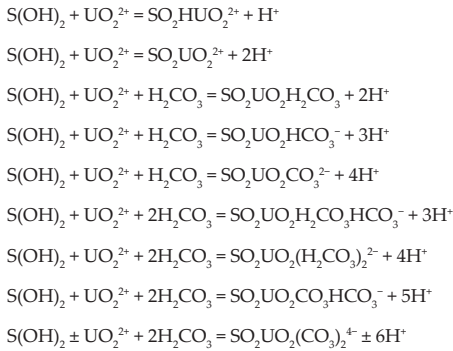
In a review, Langmuir [38] reported solution U(VI) speciation data from pH 7 groundwater at Yucca Mountain (Nevada, USA) with a total U(VI) concentration of 10^{-8} mol/L. The U(VI) percentage speciation was: (1) UO_2CO_3 at 7.9%, (2) $\text{UO}_2(\text{CO}_3)_2$ at 83.1%, (3) $\text{UO}_2(\text{CO}_3)_3$ at 7.8%, (4) UO_2F at 0.007%, (5) $\text{UO}_2(\text{OH})_2$ at 0.06% and (6) UO_2PO_4 at 0.8%. Pabalan and Turner [57] used a double layer model for simulating U(VI) adsorption on a smectite (montmorillonite). Their surface complexation constants were (1) $> \text{AlO}^-$ of -9.73 , (2) $> \text{Al}(\text{OH})_2^+$ of 8.33 , (3) $> \text{SiO}^-$ of -7.20 , (4) $\text{AlO}-\text{UO}_2^+$ of 2.70 , (5) $> \text{SiO}-\text{UO}_2^+$ of 2.60 , (6) $\text{AlO}-(\text{UO}_2)_3(\text{OH})_5$ of -14.95 and (7) $\text{SiO}-(\text{UO}_2)_3(\text{OH})_5$ of -15.29 .

Uranium(VI) may be adsorbed onto Fe-oxyhydroxides which may subsequently pursue distinctive pathways: (1) U(VI) undergoes reduction to U(IV) by mobile Fe^{2+} or H_2S or (2) desorbed, especially in alkaline solutions at elevated pH levels. Surface properties of soil mineral phases have altered chemical's reactivity because of the presence of small quantities of noncrystalline Fe- and Al-oxyhydroxides. Thus, these alterations of chemical affinity may be attributed to differences in surface area, abundance and composition of Al-OH, Fe-OH and Si-OH groups, and other features that impact the structure of adsorption surfaces (Table 11 and 12).

	Log K for ≡Al	Log K for ≡Si
$\text{SOH} + \text{H}^+ = \text{SOH}_2^+$	12.3	-0.95
$\text{SOH} = \text{SO}^- + \text{H}^+$	-13.6	-6.95
$\text{SOH} + \text{UO}_2^{2+} = \text{SO}-\text{UO}_2^+ + \text{H}^+$	7.1	0.15
$\text{SOH} + (\text{UO}_2)_3(\text{OH})_5^+ = \text{SO}-(\text{UO}_2)_3(\text{OH})_5 + \text{H}^+$	-15.8	-16.80

S is the surface site representing Al and Si.

Table 11. Adsorption site reactions and surface protonation/deprotonation reactions (McKinley et al. [46]).



where $S(\text{OH})_2$ is the surface site.

Table 12. Surface reactions on surface adsorption modeling (Herbelin and Westall [74]).

Davis et al. [44] used the generalized composite model with variations of defining equilibria to model adsorption scenarios of UO_2^{2+} onto mixed mineralogy samples from the Koongarra W2 (Australia) U-impacted samples. The UO_2^{2+} initial equilibration concentration was 3.9×10^{-6} mole U/L with variable CO_2 partial pressures. Given the different model equilibrium constraints, in general, the adsorption species dominance was (1) SO_2UO_2 (pH 5.2–5.6), (2) $\text{SO}_2\text{UO}_2\text{CO}_3^{2-}$ (pH 8.3–8.5), (3) $\text{SO}_2\text{UO}_2\text{CO}_3\text{HCO}_3^{3-}$ (pH 7.5–8.7), (4) $\text{SO}_2\text{UO}_2\text{HCO}_3^{1-}$ (pH 6.5–7.8), (5) $\text{SO}_2\text{UO}_2(\text{HCO}_3)^{3-}$ (pH \approx 8) and (6) SO_2HUO_2 (pH \approx 6), where S is the surface site.

Waite et al. [58] investigated U(VI) adsorption onto ferrihydrite as a function of U(VI) concentration and the partial pressure of CO_2 . Using the diffuse double layer model with two site surface complexes (weak and strong $\equiv\text{FeOH}$), they hypothesized that UO_2 and at higher pH levels, $\text{UO}_2(\text{CO}_3)$ formed inner sphere mononuclear, bidentate complexes involving the Fe octahedron edge and the uranyl ion. The U-interacting surface reactions without CO_2 participation were $[\equiv\text{Fe}(\text{OH})_2] + \text{UO}_2^{2+} = [\text{FeO}_2]\text{UO}_2 + 2\text{H}^+$ with $\log K = -2.57$ for the strong site and $\log K = -6.28$ for the weak site. The U-interacting surface reactions with CO_2 participation were $[\equiv\text{Fe}(\text{OH})_2] + \text{UO}_2^{2+} + \text{CO}_2 = [\text{FeO}_2]\text{UO}_2\text{CO}_3^{2-} + 2\text{H}^+$ with $\log K = 3.67$ for the strong site and $\log K = -0.42$ for the weak site.

McKinley et al. [46] observed U(VI) hydrolysis and adsorption onto smectite (SWy-1) at three ionic strengths over a pH range of 4.0–8.5. At low ionic strength, U(VI) adsorption decreased from pH 4 to pH 7, whereas at higher ionic strengths, U(VI) adsorption increased with increasing pH, an attribute attributed to uranyl hydrolysis and cation exchange involving the background electrolyte. Aluminol surface sites were dominant with adsorption of UO_2^{2+} , whereas $(\text{UO}_2)_3(\text{OH})_5^+$ was important in alkaline pH on SiOH edge sites. Turner et al. [49] employed a composite model based on gibbsite ($\alpha\text{-Al}(\text{OH})_3$) and silica ($\alpha\text{-SiO}_2$) equilibrations under similar experimental conditions to investigate U(VI) adsorption onto ferruginous beidellite (smectite family) over a pH range from 4.0 to 10.0. The adsorption envelopes for both Al (gibbsite) and Si (silica) began near pH 4 and declined near pH 5.5. With the U(VI) concentration established at UO_2 at 10^{-7} mol U/L, the model predicted the U aqueous species to be

UO_2 , $\text{UO}_2(\text{OH})^+$, $\text{UO}_2(\text{OH})_2$ and $\text{UO}_2(\text{OH})_3^-$. At UO_2 at 10^{-5} mol U/L, the model predicted the U aqueous species to be the same U species at 10^{-7} mol U/L with the addition of $(\text{UO}_2)_2(\text{OH})_2^{2+}$, $(\text{UO}_2)_3(\text{OH})_5^+$, $(\text{UO}_2)_4(\text{OH})_7^+$ and $(\text{UO}_2)_3(\text{OH})_7^{1-}$. The sorption site species were proposed as $\text{SiO}(\text{UO}_2)_3(\text{OH})_5$ and $\text{SiO}(\text{UO}_2)^+$ at Si sites and $\text{AlO}(\text{UO}_2)_3(\text{OH})_5$ and $\text{AlO}(\text{UO}_2)^+$ at Al sites.

Gao et al. [75] investigated U(VI) sorption on kaolinite using batch experiments to observe the effects of pH, U(VI) concentration and the presence of oxyanions. The sorption of U(VI) on kaolinite increased with pH increases from pH 4.0 to pH 6.5, thereafter, a sorption plateau was indicated. The presence of phosphate increased U(VI) sorption, especially in the pH range from pH 3.0 to pH 6.0, whereas sulfate had no measurable influence. UO_2HPO_4 is predicted as the major U(VI)-phosphate species from pH 4.0 to pH 6.0, thus, the sorption promotion effect of phosphate was attributed to $[\equiv\text{SOH} + \text{UO}_2^{2+} + \text{HPO}_4^{2-} = \equiv\text{SOUO}_2\text{HPO}_4^- + \text{H}^+]$.

Barnett et al. [41] observed that U(VI) adsorption on naturally occurring media of mixed mineralogy was nonlinear, suggesting that preferential and finite binding sites exist. Adsorption increased strongly with pH transition from pH 4.5 to pH 5.5 and decreased sharply from pH 7.5 to pH 8.5. The reduced adsorption was associated with carbonate-U(VI) complexes. Hummel et al. [76] provided an excellent companion thermochemical database. The MinteqA2 is able to perform adsorption simulations using: (1) Langmuir, (2) ion-exchange, (3) triple layer, (4) Freundlich, (5) constant capacitance and (6) diffuse layer [59].

Author details

Michael Thomas Aide

Address all correspondence to: mtaide@semo.edu

Department of Agriculture, Southeast Missouri State University, Cape Girardeau, Missouri, USA

References

- [1] Greenwood NN, Earnshaw A. Chemistry of the Elements. New York: Pergamon Press; 1984
- [2] Keller C. Radiochemistry. Ellis Horwood Series in Physical Chemistry. Chichester, UK: Ellis Horwood Limited; 1988
- [3] Wanty RB, Nordstrom DK. Natural radionuclides. In: Alley WM, editor. Regional Ground-Water Quality. New York: Van Nostrand Reinhold; 1995
- [4] Aide MT, Beighley D, Dunn D. Soil profile thorium and uranium concentration distribution in southeastern Missouri soils. In: Jamison R, editor. Thorium, Chemical Properties, Uses, and Environmental Effects. NY: NOVA Publishers; 2014

- [5] Birke M, Rauch U, Lorenz H. Uranium in stream and mineral water of the Federal Republic of Germany. *Environmental Geochemistry and Health*. 2009;**31**:693-706
- [6] Mendez-Garcia CG, Luna-Porres MY, Montero-Cabrera ME, Renteria-Villalobos M, Perez-Cazares B, Garcia-Tenorio R. Arsenic, lead, and uranium concentrations on sediments deposited in reservoirs in the Rio Grande Basin, USA-Mexico border. *Journal of Soils and Sediments*. 2016;**16**:1970-1985
- [7] Bleise A, Danesi PR, Burkart W. Properties, use and health effects of depleted uranium (DU): A general overview. *Journal of Environmental Radioactivity*. 2003;**64**:93-112
- [8] Dowdall M, Gwynn JP, Gabrielsen GW, Lind B. Assessment of elevated radionuclide levels in soils associated with an avian colony in a high arctic environment. *Soil and Sediment Contamination*. 2005;**14**:1-11
- [9] Graham MC, Oliver IW, MacKenzie AB, Ellam RM, Farmer JG. Mechanisms controlling lateral and vertical pore-water migration of depleted uranium (DU) at two UK weapons testing sites. *Science of the Total Environment*. 2011;**409**:1854-1866
- [10] Hamby DM, Tynybekov AK. Uranium, thorium, and potassium in soils along the shore of Lake Issyk-Kyol in the Kyrgyz Republic. *Environmental Monitoring and Assessment*. 2002;**73**:101-108
- [11] Handley-Sidhu S, Keith-Roach MJ, Lloyd JR, Vaughan DJ. A review of the environmental corrosion, fate and bioavailability of munitions grade depleted uranium. *Science of the Total Environment*. 2010;**408**:5690-5700
- [12] Kratz S, Chung E. Rock phosphate and P-fertilizers as sources of P contamination in agriculture soils. In: Merkel BJ, Hasche-Berger A, editors. *Uranium in the Environment*. Berlin: Springer; 2006. pp. 57-68
- [13] Morton LS, Evans CV, Estes GO. Natural uranium and thorium distributions in podzolized soils and native blueberry. *Journal of Environmental Quality*. 2002;**31**:155-162
- [14] Raju KK, Raju AN. Biogeochemical investigation in south eastern Andhra Pradesh: The distribution of rare earths, thorium and uranium in plants and soils. *Environmental Geology*. 2000;**39**:1102-1106
- [15] Rivas MDC. Interactions between soil uranium contamination and fertilization with N, P, and S on the uranium content and uptake of corn, sunflower, and bean and soil microbiological parameters. In: *Landbauforschung Volkenrode Sonderheft 287*. Germany: Braunschweig; 2005
- [16] Roh Y, Lee SR, Choi SK, Elless MP, Lee SY. Physicochemical and mineralogical characterization of uranium-contaminated soils. *Soil and Sediment Contamination*. 2000;**9**:463-486
- [17] Stojanovic MD, Stevanovic DR, Milojkovic JV, Grubisic MS, Lies DA. Phytotoxic effect of uranium on the growing up and development the plant of corn. *Water, Air, and Soil Pollution*. 2010;**209**:401-410

- [18] Stojanovic M, Stevanovic D, Milojkovic J, Mihajlovic ML, Lopacic Z, Sostaric T. Influence of soil type and physical-chemical properties on uranium sorption and bioavailability. *Water, Air, and Soil Pollution*. 2012;**223**:135-144
- [19] Varinlioglu A, Kose A. Determination of natural and artificial radionuclide levels in soils of western and southern coastal area of Turkey. *Water, Air, Soil Pollution*. 2005; **164**:401-407
- [20] Echevarria G, Sheppard IM, Morel JL. Effect of pH on the sorption of uranium in soils. *Journal of Environmental Radioactivity*. 2001;**53**:257-264
- [21] Laroche L, Henner P, Camilleri V, Morello M, Garnier-Laplace L. Root uptake of uranium by a higher plant model (*Phaseolus vulgaris*) – Bioavailability from soil solution. *Radioprotection*. 2005;(40):33-39
- [22] Bhattacharyya P, Datta SC, Dureja P. Interrelationship of pH, organic acids, and phosphorus concentration in soil solution of rhizosphere and non-rhizosphere of wheat and rice crops. *Communications in Soil Science and Plant Analysis*. 2003;**34**:231-245
- [23] Daquene L, Vandenhove H, Tack F, Van der Avoort E, Wannijn J, Van Hees M. Phytoavailability of uranium: Influence of plant species and soil characteristics. In: Merkel BJ, Hasche-Berger A, editors. *Uranium in the Environment*. Berlin: Springer; 2006
- [24] Daquene L, Van Hees M, Baeten E, Wannijn J, Vandenhove H. Effect of biodegradable amendments on uranium solubility in contaminated soils. *Science of the Total Environment*. 2008;**391**:26-33
- [25] Daquene L, Vandenhove H, Tack F, Meers E, Baeten J, Wannijn J. Enhanced phytoextraction of uranium and selected heavy metals by Indian mustard grass and ryegrass using biodegradable soil amendments. *Science of the Total Environment*. 2009;**407**:1495-1505
- [26] Entry JA, Vance NC, Hamilton MA, Zabowski D, Watrud LS, Adriano DC. Phytoremediation of soil contaminated with low concentrations of radionuclides. *Water, Air, and Soil Pollution*. 1996;**88**:167-176
- [27] Huang FYC, Brady PV, Lindgren ER, Guerra P. Biodegradation of uranium-citrate complexes: Implications for extraction of uranium from soils. *Environmental Science & Technology*. 1998;**32**:379-382
- [28] Huang JW, Blaylock MJ, Kapulnik Y, Demsley BBD. Phytoremediation of uranium-contaminated soils: Role of organic acids in triggering uranium hyperaccumulation in plants. *Environmental Science & Technology*. 1998;**32**:2004-2008
- [29] Sevostianova E, Lindermann WC, Ulery AL, Remmenga MD. Plant uptake of depleted uranium from manure-amended and citrate treated soil. *International Journal of Phytoremediation*. 2010;**12**:550-561
- [30] Sheppard MI, Sheppard SC, Thibault. Uptake by plants and migration of uranium and chromium in field lysimeters. *Journal of Environmental Quality*. 1984;**13**:357-361

- [31] Ebbs SD, Brady DJ, Kochian LV. Role of uranium speciation in the uptake and translocation of uranium by plants. *Journal of Experimental Botany*. 1998;**49**:1183-1190
- [32] Ebbs SD, Norvell WA, Kochian LV. The effect of acidification and chelating agents on the solubilization of uranium from contaminated soil. *Journal of Environmental Quality*. 1998;**27**:1486-1494
- [33] Shahandeh H, Hossner LR. Role of soil properties in phytoaccumulation of uranium. *Water, Air, and Soil Pollution*. 2002;**141**:165-180
- [34] Kumar A, Singhal RK, Preetha J, Rupali K, Narayanan U, Suresh S, Mishra MK, Ranade AK. Impact of tropical ecosystem on the migrational behavior of K-40, Cs-137, Th-232 and U-238 in perennial plants. *Water, Air, and Soil Pollution*. 2008;**192**:293-302
- [35] Chopping PM, Shanbhag GR. Binding of uranyl to humic acid. *Journal of Inorganic and Nuclear Chemistry*. 1981;**43**:3369-3374
- [36] Essington M. *Soil and Water Chemistry: An Integrative Approach*. Boca Raton, FL: CRC Press; 2004
- [37] Moon JW, Roh Y, Phelps TJ, Phillips DH, Watson DB, Kim YJ, Brooks SC. Physiochemical and mineralogical characterization of soil-saprolite cores from a research site, Tennessee. *Journal of Environmental Quality*. 2006;**35**:1731-1741
- [38] Langmuir D. *Aqueous environmental geochemistry*. Upper Saddle River, New Jersey: Prentiss-Hall; 1997
- [39] Sato T, Murakami T, Yanase N, Isobe H, Payne TE, Airy P. Iron nodules scavenging uranium from ground water. *Environmental Science & Technology*. 1997;**31**:2854-2858
- [40] Chen JP, Yiacoumi S. Modeling of depleted uranium transport in subsurface systems. *Water, Air and Soil Pollution*. 2002;**140**:173-201
- [41] Barnett MO, Jardine PM, Brooks SC, Selim HM. Adsorption and transport of uranium (VI) in subsurface media. *Soil Science Society of America*. 2000;**64**:908-917
- [42] Barnett MO, Jardine PM, Brooks SC. Uranium(VI) adsorption to heterogeneous subsurface media: Application of a surface complexation model. *Environmental Science & Technology*. 2002;**36**:937-942
- [43] Cygan RT. Molecular models of radionuclide interaction with soil minerals. In: Zhang P-C, Brady PV, editors. *Geochemistry of Soil Radionuclides*. Soil Science Society America Special Publication 59. Madison, WI: Soil Science Society America; 2002
- [44] Davis JA, Payne TE, Waite TD. Simulating the pH and pCO₂ dependence of uranium(VI) adsorption by a weathered schist with surface complexation models. In: Zhang P-C, Brady PV, editors. *Geochemistry of Soil Radionuclides*. Soil Science Society America Special Publication 59. Madison, WI: Soil Science Society America; 2002
- [45] Honeyman BD, Ranville JF. Colloid properties and their effects on radionuclide transport through soils and groundwaters. In: Zhang P-C, Brady PV, editors. *Geochemistry*

of Soil Radionuclides. Soil Science Society America Special Publication 59. Madison, WI: Soil Science Society America; 2002

- [46] McKinley JP, Zachara JM, Smith SC, Turner GD. The influence of uranyl hydrolysis and multiple site-binding reactions on the adsorption of U(VI) to montmorillonite. *Clays and Clay Minerals*. 1995;**43**:586-598
- [47] Runde W. Geochemical interactions of actinides in the environment. In: Zhang P-C, Brady PV, editors. *Geochemistry of Soil Radionuclides*. Soil Science Society America Special Publication 59. Madison, WI: Soil Science Society America; 2002
- [48] Runde W, Neu MP, Conradson SD, Li D, Lin M, Smith DM, Van-Pelt CE, Xu Y. Geochemical speciation of radionuclides in soil and solution. In: Zhang P-C, Brady PV, editors. *Geochemistry of Soil Radionuclides*. Soil Science Society America Special Publication 59. Madison, WI: Soil Science Society America; 2002
- [49] Turner GD, Zachara JM, McKinley JP, Smith SC. Surface charge properties and UO_2^{2+} adsorption on a subsurface smectite. *Geochimica et Cosmochimica Acta*. 1996;**60**: 3399-3414
- [50] Bidoglio G, De Plano A, Righetto L. Interaction and transport of plutonium-humic acid particles in groundwater environments. *Materials Research Society Symposium Proceedings*. 1989;**127**:823-830
- [51] Johnson WH, Buck BJ, Brogonia H, Brock AL. Variations in depleted uranium sorption and solubility with depth in arid soils. *Soil and Sediment Contamination*. 2004;**13**:533-544
- [52] Martinez-Aguirre A, Perianez R. Sedimentary speciation of U and Th isotopes in a marsh area at the southwest of Spain. *Journal of Radioanalytical and Nuclear Chemistry*. 2001;**247**:45-52
- [53] Baes CF, Mesmer RE. *The Hydrolysis of Cations*. N.Y: Wiley-Interscience; 1976
- [54] Davis JA. Surface complex modeling of uranium(VI) adsorption on natural mineral assemblages. In: NUREG/CR-6708. Washington DC: U.S. Nuclear Regulatory Commission; 2001
- [55] Grenthe I, Fuger J, Lemire R, Muller AB, Nguyen-Trung C, Wanner H. *Chemical Thermodynamics of Uranium*. France: OECD Nuclear Energy Agency (NEA); 1992
- [56] Hsi C-KD, Langmuir D. Adsorption of uranyl onto ferric oxyhydroxides: Application of the surface complexation site binding model. *Geochimica et Cosmochimica Acta*. 1985;**49**:1931-1941
- [57] Pabalan RT, Turner DR. Uranium(6+) sorption on montmorillonite: Experimental and surface complexation modeling study. *Aqueous Geochemical*. 1997;**2**:203-226
- [58] Waite TO, Davis JA, Payne TE, Waychunas GA, Xu N. Uranium (VI) adsorption to ferrihydrate: Application of a surface complexation model. *Geochimica et Cosmochimica Acta*. 1994;**58**:5465-5478

- [59] Allison JD, Brown DS, Novo-Gradac KL. Minteqa2/Prodefa2, a Geochemical Assessment Model for Environmental Systems: Version 3.0. Athens, GA: Environmental Research Laboratory, Office of Research and Development, USEPA; 1991
- [60] Stewart BD, Neiss J, Fendorf S. Quantifying constraints imposed by calcium and iron on bacterial reduction of uranium(VI). *Journal of Environmental Quality*. 2007;**36**:363-372
- [61] Yajima T, Kawamura Y, Ueta S. Uranium(IV) solubility and hydrolysis constants under reduced conditions. *Materials Research Society Symposium Proceedings*. 1995;**333**: 1137-1142
- [62] Goldhaber MB, Hemingway BS, Mohagheghi A, Reynolds RL, Northrop HR. Origin of coffinite in sedimentary rocks by a sequential adsorption reduction mechanism. *Bulletin de Mineralogie*. 1987;**110**:131-141
- [63] Fendorf S, Hansel CM, Wielinga. Operative pathways of chromate and uranyl reduction within soils and sediments. In: Zhang P-C, Brady PV, editors. *Geochemistry of Soil Radionuclides*. Soil Science Society America Special Publication 59. Madison, WI: Soil Science Society America; 2002
- [64] Burgos WD, Senko JM, Dempsey BA, Roden EE, Stone JJ, Kemner KM, Kelly SD. Soil humic acid decreases biological uranium(VI) reduction by *Shewanella putrefaciens* CN32. *Environmental Engineering Science*. 2007;**24**:755-761
- [65] Grabias E, Gladysz-Plaska A, Ksiazek A, Majdan M. Efficient uranium immobilization on red clay with phosphates. *Environmental Chemistry Letters*. 2014;**12**:297-301
- [66] Jerden LJ, Sinha KA. Phosphate based immobilization of uranium in an oxidizing bed-rock aquifer. *Applied Geochemistry*. 2003;**18**:823-843
- [67] Mehta VS, Giammar DE, Maillot F, Catalano JG, Wang Z. Transport of U(VI) through sediments amended with phosphate to induce in situ uranium immobilization. *Water Research*. 2015;**69**:307-317
- [68] Sandino A, Bruno J. The solubility of $(\text{UO}_2)_3(\text{PO}_4)_2 \cdot 4\text{H}_2\text{O}$ (s) and the formation of U(VI) phosphate complexes: Their influence in uranium speciation in natural waters. *Geochimica et Cosmochimica Acta*. 1992;**56**:4135-4145
- [69] Lenhart JJ, Cabaniss SE, MacCarthy P, Honeyman BD. Uranium(VI) complexation with citric, humic and fulvic acids. *Radiochimica Acta*. 2000;**88**:345-353
- [70] Ivanov P, Griffiths T, Bryan ND, Borrhikov G, Dmitriev S. The effect of humic acid on uranyl sorption onto bentonite at trace uranium levels. *Journal of Environmental Monitoring*. 2012;**14**:2968-2975
- [71] Tinnacher RM, Nico PS, Davis JA, Honeyman BD. Effects of fulvic acid on uranium(VI) sorption kinetics. *Environmental Science & Technology*. 2013;**47**:6214-6222
- [72] Tandy S, Brittain SR, Grail BM, Mcleod CW, Paterson A, AD T. Fine scale measurement and mapping of uranium in soil solution in soil and plant-soil microcosms, with special reference to depleted uranium. *Plant and Soil*. 2013;**368**:471-482

- [73] Phillips DH, Watson DB, Roh Y, Mehlhorn TL, Moon JW, Jardine PM. Distribution of uranium in weathered fractured saprolite/shale and ground water. *Journal of Environmental Quality*. 2006;**35**:1715-1730
- [74] Herbelin AL, Westall JA. FITEQL: A computer program for the determination of chemical equilibrium constants from experimental data. Version 4.0 Rep.99-01. Oregon State Univ., Corvallis; 1999
- [75] Gao L, Yang Z, Shi K, Wang X, Guo Z, Wu W. U(VI) sorption on kaolinite: Effects of pH, U(VI) concentration and oxyanions. *Journal of Radioanalytical and Nuclear Chemistry*. 2010;**284**:519-526
- [76] Hummel W, Berner U, Curti E, Pearson FJ, Thoenen T. Nagra/PSI Chemical Thermodynamic Data Base 01/01. USA: Universal Publishers/uPUBLISH.com; 2002

